

# A discrete piezoelectric stack absorber model

C.J. Stander<sup>1</sup> and P.S. Heyns<sup>2</sup>

(First received October 2000; Final version March 2001)

Mechanical absorbers are sometimes used to reduce vibration levels on structures that are subjected to narrow band dynamic excitation. However, active control systems have in recent years received a great deal of attention and can be very effective. They are however costly. This raises the need for an intermediate solution that can provide some of the advantages, of an active system, at significantly lower cost. The passively shunted piezoelectric stack actuator is an example of such an intermediate step, between a mechanical absorber and an active control system. The device is less expensive and its adaptability is superior to that of the mechanical absorber. With this work, a mathematical model of such a device was derived and verified experimentally. The shunted piezoelectric actuator was applied to an aluminium cantilever beam and 81.7% attenuation was obtained for a tuned mode.

## Nomenclature

$A$	Area of the piezoelectric perpendicular to the poling direction
$C_A^T$	Inherent capacitance of the piezoelectric stack actuator
$C_p^T$	Inherent capacitance of the piezoelectric element
$D$	Electrical displacement
$E$	Electrical field in the material
$I$	Electrical current
$K_{ACT}$	Dynamic stiffness of the shunted piezoelectric actuator
$K_{Pre-stress}$	Stiffness due to the pre-stress on the piezoelectric elements in the actuator
$K_{Series}$	Stiffness due to end caps, electrodes and insulating layers
$K_{33}^{ME}$	Relation between the applied force and displacement for the uniaxial loading case
$L$	Length of the piezoelectric element in the poling direction
$L_i$	Electrical inductance
$R$	Electrical resistance

$S$	Material engineering strain
$S^{SU}$	Compliance of the shunted piezoelectric element
$T$	Material stress
$V$	Electrical voltage (Tension)
$Y^D$	Open circuit admittance due to the inherent capacitance of the piezoelectric element
$Y^{EL}$	Electrical admittance of the shunted piezoelectric
$Y^{SU}$	Admittance of the shunt circuit
$Z^{EL}$	Electrical impedance equal to the inverse of the electrical admittance
$\epsilon^T$	Dielectric constant
$d_{33}$	Piezoelectric constant with poling and deformation in the 3 direction
$s$	Laplace parameter
$s^E$	Piezoelectric material compliance at constant field
$\delta$	Relative displacement between the end caps of the piezoelectric stack actuator

## Introduction

Mechanical absorbers can be very useful for the attenuation of vibration on structures subjected to narrow band excitation. Recently, however, more attention has been devoted to utilising active control, since these systems can be very effective. An active vibration control system consists of transducers, actuators, amplifiers, computational devices or electrical circuitry. Therefore considerable costs may be involved in the implementation of such systems.

The actuators used in the active control of structural vibration are usually piezoelectric actuators or magnetostrictive actuators. These actuators are chosen for their high force per unit volume and operational frequency band characteristics. Although the properties of these piezoelectric and magnetostrictive actuators make them attractive for vibration attenuation, the cost of their implementation, in the active control environment, lessens this appeal.

Recent advances in the field of smart materials research have led to the implementation of these actuators as passive dampers and absorbers. The actuators are attached to a structure to alter the dynamic characteristics of the structure. A passive electrical circuit is connected in parallel to the poles of the actuators to adjust the dynamic characteristics of the actuator and hence that of the structure. The possibility of using piezoelectric materials as passive elements to attenuate vibration was first proposed by Forward<sup>1</sup> in 1979.

<sup>1</sup>Postgraduate student, Dynamic Systems Group, Department of Mechanical and Aeronautical Engineering, University of Pretoria, Pretoria, 0002 South Africa

<sup>2</sup>Professor, Dynamic Systems Group, Department of Mechanical and Aeronautical Engineering, University of Pretoria, Pretoria, 0002 South Africa

Smart actuators are used as energy couplers to convert mechanical energy into electrical energy. The electrical energy is dissipated externally in an electric circuit. The electrical circuit consists of a resistive element that is used to dissipate the electrical energy. In some of the electrical circuits an inductor is added in series to the resistive element. The addition of the inductor causes the circuit to resonate. Additional vibration attenuation can be obtained by tuning the resonant frequency.

Hagood & Von Flotow<sup>2</sup> first implemented a resistor in the shunt circuit to enhance the damping of the structure to which the piezoelectric actuator is attached. An actuator that is shunted resistively is essentially a damper and is analogous to viscoelastic materials being utilised as vibration dampers.

An actuator that is shunted resistive-inductive is analogous to a mechanically tuned damped mass absorber. The small size of the actuators and the simplicity, with which the absorption frequency can be changed, gives the concept an advantage over mechanical absorbers.

In contrast to traditional viscoelastic or viscous fluids where the energy dissipation occurs internally, smart actuators employ external dissipation. If the energy is dissipated externally, the characteristics of the attenuation device become insensitive to temperature change during the dissipation of the vibration energy.

Smith & Anderson<sup>3</sup> dealt with the selection of a suitable type of actuator for passive damping applications. The smart actuators considered in this paper were piezoelectric, electrostrictive, and magnetostrictive types. Piezoelectric actuators are the most practical to implement as passive dampers and absorbers, since the electromechanical coupling is linear and no external stimuli are required. The non-linearity of the material characteristics can usually be ignored. Magnetostrictive and electrostrictive actuators impose difficulties due to the non-linear characteristics and external stimuli.

Piezoelectric elements may be implemented in either a longitudinal or a transverse configuration. The term longitudinal refers to the instance where the deformation of the material is perpendicular to the electrodes of the element. The transverse case refers to the instance where the deformation of the material occurs in parallel with the electrodes of the element. The transverse case is often referred to as a wafer or sheet and piezoelectric stack actuator is the term used for a multi-layered longitudinal configuration co-fired into one solid. The use of piezoelectric elements in the longitudinal direction is preferred to the transverse direction for passive damping applications, since the electromechanical coupling is much higher in the longitudinal direction.

Inman<sup>4</sup> concluded that passive electronic damping has become a viable alternative to passive viscoelastic damping, whilst Browning & Woodson<sup>5</sup> indicated that it is possible to attenuate as many as twelve different modes of a steel plate with four piezoelectric wafer elements. Edberg, Bicos, Fuller & Tracy<sup>6</sup> attenuated multiple modes of a structure with a single piezoelectric wafer element.

The work in this paper was conducted to investigate the applicability of using a passively shunted piezoelectric stack actuator to attenuate structural vibration.

A mathematical model was derived for the piezoelectric stack actuator as a damped discrete absorber. The model was verified experimentally on an aluminium cantilever beam in order to determine whether it is possible to attenuate the modes of a structure with such a device and to validate the model.

## Mathematical model of the shunted piezoelectric stack actuator

Hagood & Von Flotow<sup>2</sup> proposed a shunted model for a piezoelectric element in a single layered longitudinal configuration. The model was not verified experimentally. The following derivation is based on the model that they proposed, but further extends the model to incorporate a multiple layer longitudinal configuration in the form of a stack actuator, between two discrete points on a structure, as an attenuation device.

### Derivation of the model

The constitutive relation for the material constants of a linear three-dimensional piezoelectric solid is presented as equation (1).

$$\begin{bmatrix} \bar{D} \\ \bar{S} \end{bmatrix} = \begin{bmatrix} \bar{\epsilon}^T & \bar{d} \\ \bar{d}_t & \bar{s}^E \end{bmatrix} \begin{bmatrix} \bar{E} \\ \bar{T} \end{bmatrix} \quad (1)$$

The uppercase entries in equation (1) represent vectors.  $D$  refers to the electrical displacement,  $E$  the electrical field,  $S$  the engineering strain, and  $T$  the material stress. The lower case entries are matrices that define the material properties of the element. The dielectric constants are denoted by  $\epsilon$ , the compliance by  $s^E$ , and the piezoelectric constants by  $d$ . The subscript  $t$  denotes the conventional matrix transpose and the compliance is specified under constant electrical field.

According to Hagood & Von Flotow<sup>2</sup> the material property matrices in equation (1) can be simplified to single value material properties under the following conditions: The piezoelectric element must be loaded uniaxially with a normal stress and only one pair of electrodes must be present on the element to develop the external electrical field in the same direction. The piezoelectric properties for the longitudinal application are denoted by subscript 33, which indicates that the direction of loading and electrical field development is in the 3 direction in accordance with piezoelectric convention.

$$\begin{bmatrix} D_3 \\ S_3 \end{bmatrix} = \begin{bmatrix} \epsilon_{33}^T & d_{33} \\ d_{33} & s_{33}^E \end{bmatrix} \begin{bmatrix} E_3 \\ T_3 \end{bmatrix} \quad (2)$$

To incorporate conventional concepts such as admittance and impedance into the shunting analysis, a change of variables is required. The definitions for voltage and

current are used for this purpose. The assumption is made that the field within and the electrical displacement on the surface are uniform for the piezoelectric material. The linear relationships can be defined in the Laplace domain by equations (3) and (4).

$$I(s) = sA \cdot D(s) \quad (3)$$

$$V(s) = L \cdot E(s) \quad (4)$$

$L$  denotes the length of the material in the poling directions,  $A$  the area perpendicular to the poling direction, and  $s$  the Laplace parameter. By taking the Laplace transform of equation (2) and using equations (3) and (4) to eliminate  $E$  and  $D$ , the constitutive relation for a piezoelectric in terms of the external current input and applied voltage is obtained.

$$\begin{bmatrix} I_3 \\ S_3 \end{bmatrix} = \begin{bmatrix} sAL^{-1}\epsilon^T & sAd_{33} \\ d_{33}L^{-1} & s_{33}^E \end{bmatrix} \begin{bmatrix} V_3 \\ T_3 \end{bmatrix} \quad (5)$$

The upper left partition of the constitutive relation matrix can be defined as the capacitance between the surfaces that are perpendicular to the poling direction. Therefore the constitutive relation can be written as

$$\begin{bmatrix} I_3 \\ S_3 \end{bmatrix} = \begin{bmatrix} sC_P^T & sAd_{33} \\ d_{33}L^{-1} & s_{33}^E \end{bmatrix} \begin{bmatrix} V_3 \\ T_3 \end{bmatrix} \quad (6)$$

The open circuit admittance of the piezoelectric due to the inherent capacitance with free boundary conditions is defined as

$$Y^D = sC_P^T \quad (7)$$

For shunted piezoelectric applications, a passive electrical circuit is connected in parallel with the surface electrodes of the piezoelectric element. The circuit is in parallel with the inherent capacitance of the piezoelectric element. The admittance in parallel adds and therefore the constitutive relation for a shunted piezoelectric element can be written as

$$Y^{EL} = Y^D + Y^{SU} \quad (8)$$

$$\begin{bmatrix} I_3 \\ S_3 \end{bmatrix} = \begin{bmatrix} Y^{EL} & sAd_{33} \\ d_{33}L^{-1} & s_{33}^E \end{bmatrix} \begin{bmatrix} V_3 \\ T_3 \end{bmatrix} \quad (9)$$

$Y^D$  denotes the open circuit electrical admittance of the piezoelectric element,  $Y^{SU}$  the shunting admittance, and  $Y^{EL}$  the electrical admittance of the shunted piezoelectric element.

An expression for the input current to the piezoelectric element is deduced from equation (9). The external current input is equal to zero for passive shunting applications.

$$I_3 = Y^{EL}V_3 + sAd_{33}T_3 \quad (10)$$

An expression for the voltage difference over the electrodes of the piezoelectric element, due to the applied stress, can be obtained through manipulation of equation (10) and by setting the external current in the equation equal to zero.

$$V_3 = -Z^{EL}sAd_{33}T_3 \quad (11)$$

$Z^{EL}$  denotes the electrical impedance which is equal to the inverse of the electrical admittance.

The expression for the piezoelectric element strain is deduced from equation (9).

$$S_3 = d_{33}L^{-1}V_3 + s_{33}^ET_3 \quad (12)$$

The strain of a single piezoelectric element in a piezoelectric stack actuator is equal to the strain of the entire stack. Therefore the strain of a single piezoelectric element may be expressed as displacement between the end caps of the piezoelectric stack actuator divided by the total initial length of the stack actuator. The total initial length of the actuator is expressed as the number of piezoelectric elements times the length of the elements.

$$\frac{\delta}{nL} = d_{33}L^{-1}V_3 + s_{33}^ET_3 \quad (13)$$

An expression that relates the displacement between the end caps to the stress applied to the piezoelectric stack is obtained by substituting equation (11) in to equation (13) and manipulating.

$$\delta = \{nls_{33}^E - nd_{33}^2sAZ^{EL}\}T_3 \quad (14)$$

Note that  $Z^{EL}$  represents the electrical impedance for a single piezoelectric element and its equivalent shunting circuit. However the piezoelectric stack actuator is shunted with a single electrical circuit which is in parallel with the inherent capacitance of the piezoelectric stack actuator. The admittances, of the piezoelectric element and their equivalent shunt circuits in the stack, are in parallel. The admittances in parallel adds and the sum of the admittance is equal to the admittance of the system. The system admittance is expressed in terms of the capacitance of the piezoelectric stack actuator and the admittance of the shunt circuit over the poles of the piezoelectric stack. Therefore the electrical impedance for a single piezoelectric element may be expressed in terms of the electrical impedance of the system.

$$nY^{EL} = Y_{SYS}^{EL} \quad (15)$$

$$Z^{EL} = nZ_{SYS}^{EL} \quad (16)$$

The dynamic stiffness of the shunted piezoelectric stack actuator, which relates the applied force to the relative displacement between the end caps of the actuator, can be deduced from equations (14) and (16).

$$K_{33}^{ME}(s) = \frac{A}{nls_{33}^E - n^2d_{33}^2sAZ_{SYS}^{EL}} \quad (17)$$

The dynamic stiffness does not account for the stiffness of the end caps, insulating layers and electrode plates. The stiffness of these components is in series with the dynamic stiffness of the piezoelectric stack. According to Shibo *et al.*<sup>7</sup> the stiffness of the pre-stress on the piezoelectric stack is in parallel with the stiffness of the piezoelectric stack. Therefore the dynamic stiffness of the shunted piezoelectric stack actuator may be written in the form of equation (18).

$$K_{ACT}(s) = \left[ \frac{1}{K_{33}^{ME}(s)} + \frac{1}{K_{Series}} \right]^{-1} + K_{Pre-stress} \quad (18)$$

By altering the electrical impedance term of the system, the passive characteristics of the piezoelectric stack actuator are altered. The process of altering the passive characteristics of the actuator has been referred to as shunting. As indicated in the introduction there are two common types of electrical networks that are used for shunting the actuator: The first which is resistive shunting, where a resistor is placed in parallel over the actuator poles, and the second where an inductor is added in series with the resistance. The second shunt is referred to as a resonant shunt.

The expression of system electrical impedance for the resistively shunted actuator is given by equation (19) and for the resonant shunted actuator by equation (20).

$$Z_{SYS}^{EL}(s) = \frac{R}{RC_A^T s + 1} \quad (19)$$

$$Z_{SYS}^{EL}(s) = \frac{L_i s + R}{L_i C_A^T s^2 + RC_A^T s + 1} \quad (20)$$

The actuator can be implemented as a damper or a damped absorber on a structure. The dynamic stiffness of the shunted piezoelectric actuator is used as a transfer function in a feedback loop to the force input of the structural model. The transfer function is obtained by substituting either equation (19) or (20) into equation (18).

The objective was set to develop a model for the shunted piezoelectric stack actuator that could be implemented within commercial software, which extracts a state space model from modal analysis measurements. However the software limits the user to displacement output in the time domain.

Therefore viscous damping can not be implemented in the feedback loop, since velocity feedback is unavailable. The resistance value in the shunt circuit is therefore increased in order to compensate for the inherent structural damping in the piezoelectric stack actuator.

### Experimental verification of the mathematical model

A piezoelectric stack actuator was connected to an aluminium cantilever beam in order to conduct the experimental verification. An experimental modal analysis was conducted on the beam in the vertical direction. The objective was to measure the influence of the shunted stack actuator on the frequency response function of the system.

An IMV Vibropet electrodynamic shaker was used to induce a random excitation force on to the beam during the modal analysis. A photo image of the experimental set-up is shown in Figure 3 and a schematic diagram is shown in Figure 4.

The equipment used during the experiments is tabulated in Table 1. Table 2 specifies the geometric information of the aluminium beam used during the experiment.

**Table 2** Dimensions of the aluminium beam

Dimension	mm
Length	490
Height	10
Width	30

The shunt circuit comprised a variable resistance potentiometer and a number of custom built inductors. The inductors were wound on ferromagnetic E cores with a current rating of 1 A. The inductance values of the various inductors were specified so that any inductance value between  $1 \times 10^{-3}$  H and 1 H could be obtained in discrete steps of  $1 \times 10^{-3}$  H by connecting the various inductors in series.

A finite element model of the beam was built with twenty Bernoulli-Euler elements and was updated with experimental data. The Experimental and Analytical Structural Dynamic Toolbox by Etienne Balnès was used in the analysis.

**Table 1** Modal measurement equipment list

Item No.	Item	Model
1	DSP Siglab signal processor and generator	20-42
2	IMV Vibropet electrodynamic shaker	PET-01
3	Rotel amplifier	RA-970BX
4	PCB miniature high frequency accelerometer	353B17
5	PCB impedance head	288D01
6	PCB battery-powered signal conditioner	480E09
7	Notebook computer	Intel 486 DX2-66
8	Piezomechanik piezoelectric stack actuator	Pst 500/5/15 VS10

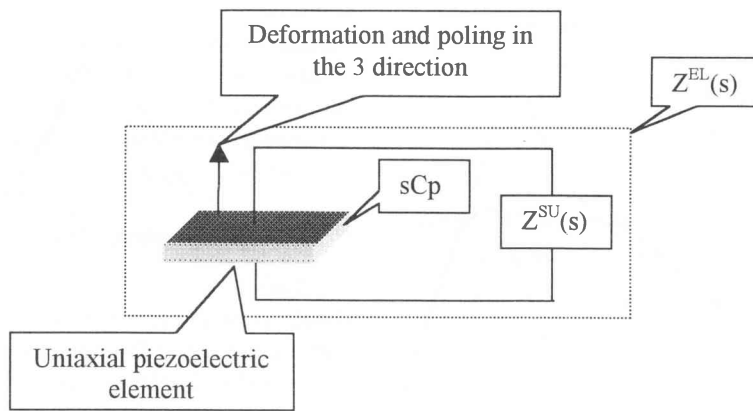


Figure 1 Schematic diagram of the shunted uniaxial piezoelectric element

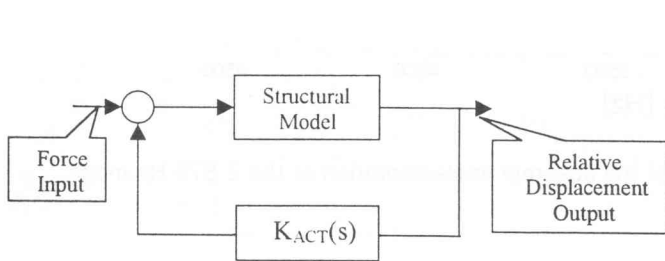


Figure 2 Flow diagram of the closed loop system

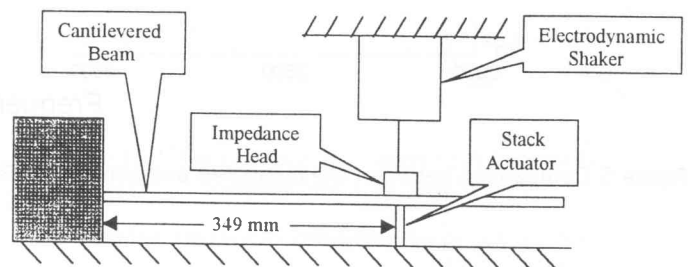


Figure 4 Graphical representation of the experimental set up

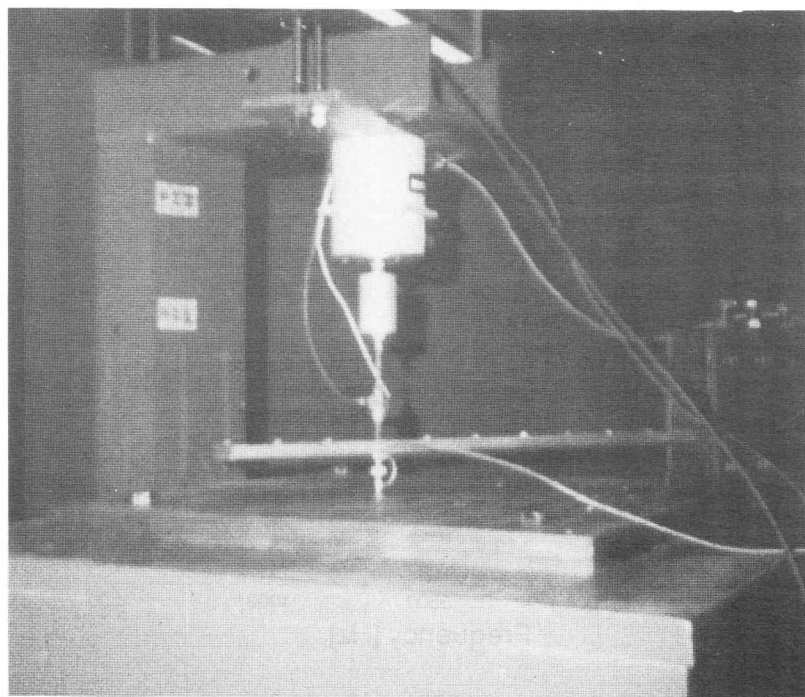


Figure 3 Experimental verification test rig

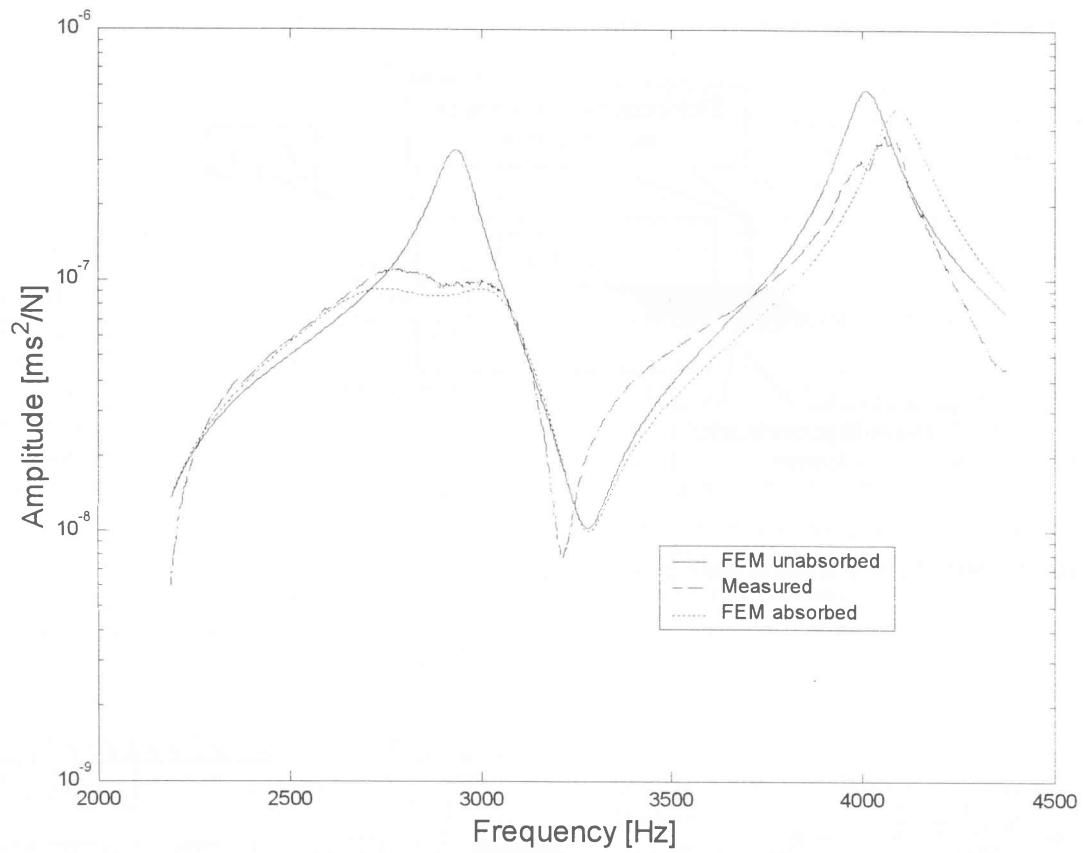


Figure 5 Comparison between the measured and simulated FRFs of the absorber implementation at the 2 875 Hz mode

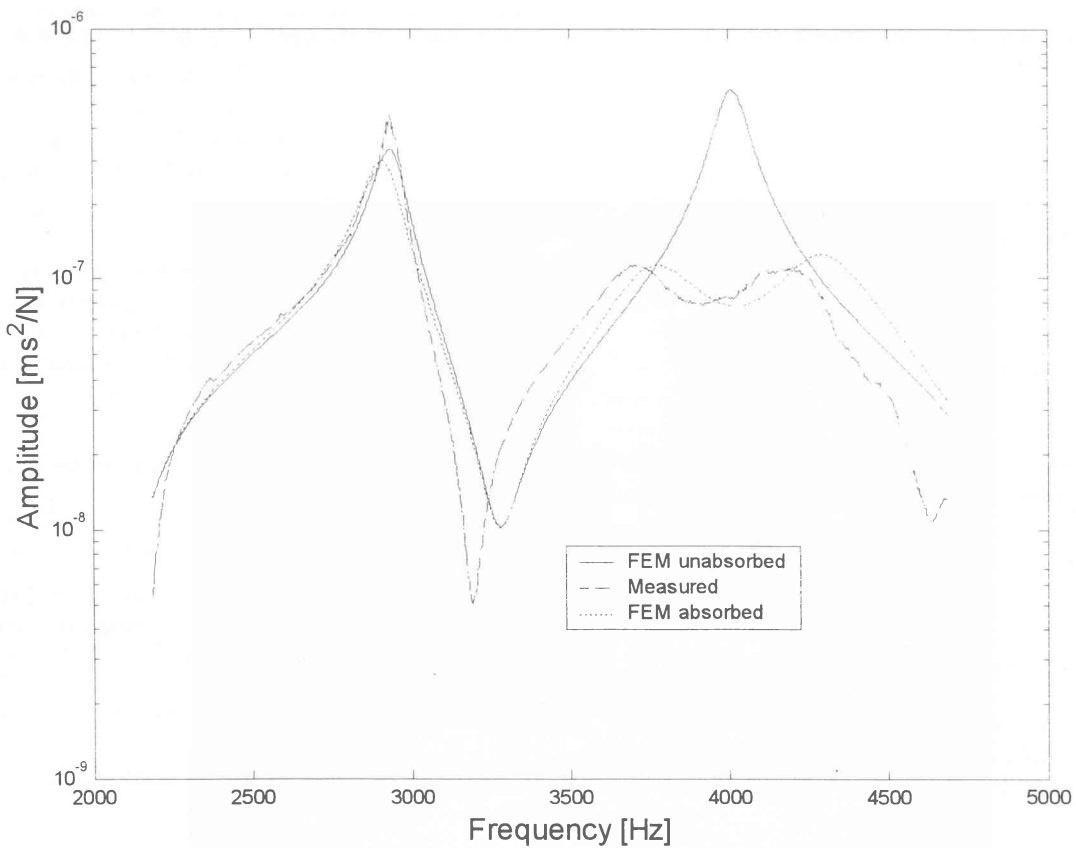


Figure 6 Comparison between the measured and simulated FRFs of the absorber implementation at the 3 910 Hz mode

This was accomplished by the use of an optimisation algorithm that implements a simplex search method. Such an approach is robust and can handle discontinuities in the objective function. The objective function was written as the sum of the absolute differences between the natural frequencies of the modes identified by the modal assurance criterion. The objective of the optimisation was to minimise the objective function. The modulus of elasticity, the material density, the beam thickness and the width of the beam were used as variable parameters in the process of updating the finite element model.

The series stiffness, parallel stiffness and shunt resistance of the actuator were used as variable parameters in a second model updating process in order to simulate the incorporation of the piezoelectric stack actuator in to the structure.

The inherent structural damping of the structure is increased when the actuator, without the shunt, is added to the structure. The feedback loop does not account for the increase in structural damping. The updating process indicated that a 50  $\Omega$  increase in the shunt circuit resistance is required to compensate for the inherent structural damping within the piezoelectric material and actuator casing.

The parameters of the mathematical model were updated to match the measured experimental results in a frequency bandwidth between 2200 Hz and 4400 Hz. Priority was given to the 11th and 13th modes since these were the modes that were selected for attenuation in the experimental verification. The frequencies and system parameters are tabulated in Table 3.

Figures 5 and 6 show the frequency response function results of the updated FEM model with and without the resonant shunt circuit coupled to the actuator poles. The frequency response functions, which were measured during the modal analysis with the resonant circuit coupled to the poles of the actuator, are presented in the figures. The optimum attenuation results are shown in Table 3 and the specifications of the Piezomechanik piezoelectric actuator are tabulated in Table 4.

### Conclusion

A mathematical model of a damped discrete piezoelectric stack absorber was derived and verified experimentally by fixing the absorber to a cantilever beam in order to attenuate its structural modes. The implementation of the damped discrete piezoelectric absorber was successful and

81.7% attenuation was obtained at one of the modes during the experimental verification.

**Table 4** Material properties of the Piezomechanik 500/5/15 piezoelectric stack actuators

Relative dielectric constant	4000
Piezoelectric charge constant	$500 \times 10^{-12}$ [m/V]
Layer thickness	$3.5 \times 10^{-4}$ [m]
Active actuator length	$15 \times 10^{-3}$ [m]
Layer diameter	$5 \times 10^{-3}$ [m]
Pre-stress stiffness	$600 \times 10^6$ [N/m]
Parallel stiffness	$1.2 \times 10^7$ [N/m]
Capacitance	$38.5 \times 10^{-9}$ [F]
Modulus of elasticity	$60 \times 10^9$ [N/m <sup>2</sup> ]

### References

1. Forward RL. Electronic damping of vibration in optical structures. *Journal of Applied Optics*, 1979, **18**, pp.690–697.
2. Hagood NW & Von Flotow A. Damping of structural vibration with piezoelectric materials and passive electrical networks. *Journal of Sound and Vibration*, 1991, **146**, pp.243–268.
3. Smith CA & Anderson EH. Passive damping by smart materials: analysis and practical limitations. *SPIE*, **2445**, pp.136–148.
4. Inman DJ. Smart structural solutions to vibration problems. *ISMA23 International Conference on Noise and Vibration Engineering*, 1998, Catholic University of Leuven, Belgium.
5. Browning DR & Woodson DW. Multiple-mode piezoelectric passive damping experiments for elastic plates. *Proceedings of the 11th International Modal Analysis Conference*, 1993, Kissimmee, pp.1520–1526.
6. Edburg DL, Bicos AS, Fuller CM & Tracy JJ. Theoretical and experimental studies of a truss incorporating active members. *Journal of Intelligent Material Systems and Structures*, 1992, **3**, pp.333–347.
7. Shibo X, Junbao L & Lingmi Z. Design modelling and verification of a piezoelectric actuator for adaptive truss structures. *Proceedings of the 15th International Modal Analysis Conference*, 1997, pp.1865–1870.

**Table 3** Experimental verification results and system parameters

Modal frequency [Hz]	Attenuation [%]	Experimental resistance value [ $\Omega$ ]	Model resistance value [ $\Omega$ ]	Experimental inductance value at 1000 Hz [H]	Model inductance value [H]
2875	77.9	100.0	100 + 50	0.0461	0.046
3910	81.7	230.0	230 + 50	0.0808	0.089